CHAPTER

139

Bionic Baroreflex

Takayuki Sato, André Diedrich, Kenji Sunagawa

A novel therapeutic strategy against central baroreflex failure is proposed based on bionic technology. The bionic baroreflex system is a recent innovation designed to revitalize baroreflex function. In the bionic baroreflex system, arterial pressure is sensed via a micromanometer placed in the aortic arch. Its output is fed into a computer that functions as an artificial vasomotor center. Based upon measured changes in arterial pressure, the artificial vasomotor center generates command signals to an electrical stimulator to provide an appropriate frequency of stimulation to vasomotor sympathetic nerves. Although the bionic baroreflex system is not currently available for clinical practice, its clinical use is expected after further development.

INTRODUCTION

The arterial baroreflex is the most important negative feedback system to suppress rapid daily disturbances in arterial pressure [1]. Therefore, in patients with autonomic failure with dysfunctional baroreflex control of arterial pressure, the simple act of standing would cause a fall in arterial pressure, reducing perfusion of the brain, and resulting potentially in loss of consciousness. The functional restoration of the arterial baroreflex is essential in numerous patients groups (e.g., those with autonomic failure) for maintaining consciousness and a level of life quality.

In patients with central baroreflex failure such as baroreceptor deafferentation, Shy–Drager syndrome, and spinal cord injuries, peripheral sympathetic nerves remain functional but are not controlled by the brain. A novel therapeutic strategy has been proposed to use a bionic baroreflex system (BBS) with a neural interface to control arterial pressure [2,3]. A bionic system is an artificial device for the functional replacement of a failed physiological system. It is should be able to mimic its static and dynamic characteristics. In the proposed BBS (Fig. 139.1), arterial pressure is sensed via a micromanometer placed in the aortic arch, and fed into a computer that functions as an artificial vasomotor center. Based upon measured changes in arterial pressure, the artificial vasomotor center generates commands signals that trigger an electrical stimulator to provide a stimulus of the appropriate frequency to vasomotor sympathetic nerves. The BBS has been able to revitalize baroreflex function in an animal model of central baroreflex failure.

BIONIC BAROREFLEX SYSTEM

Theoretical Background

It is of critical importance to identify the algorithm of the artificial vasomotor center, i.e., how to determine the stimulation frequency (STM) of the vasomotor sympathetic nerves in response to a change in arterial pressure (AP). Based on expertise of bionics and systems physiology, the algorithm has been determined as a transfer function by using a white-noise identification method [2]. First, the functional characteristics have to be mimicked by the BBS, i.e., the open-loop transfer function of the native baroreflex

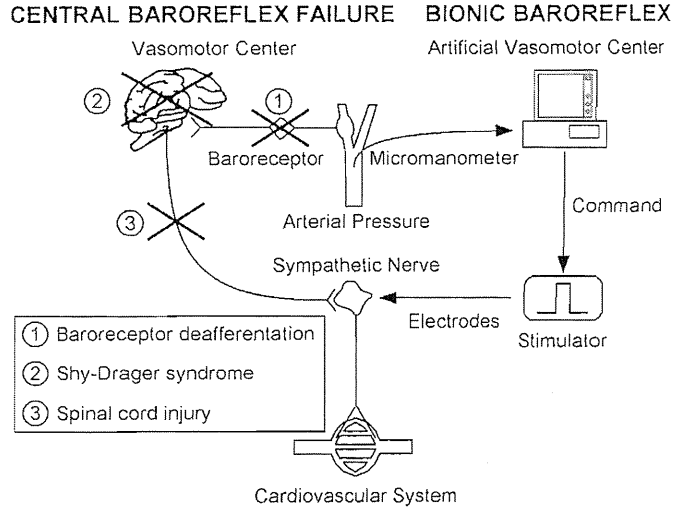

FIGURE 139.1 Central baroreflex failure and its functional replacement by a bionic baroreflex system.

Primer on the Autonomic Nervous System. DOI: 10.1016/B978-0-12-386525-0.00139-6

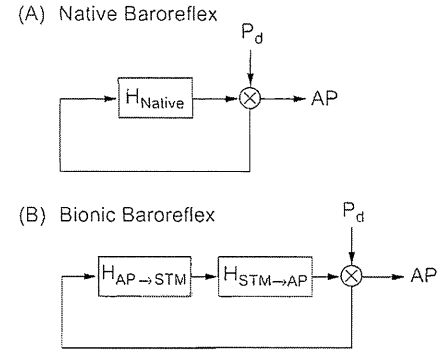

FIGURE 139.2 Block diagrams of native and bionic baroreflex systems. HNative denotes the open-loop transfer function of the native baroreflex system. H_{AP-STM} and H_{STM-AP} are the open-loop transfer functions from arterial pressure (AP) to the frequency of electrical stimulation (STM) and from STM to AP, respectively. P_d is an external disturbance in pressure. *(Modified from Sato et al. (2002) with permission of American Heart Association.)*

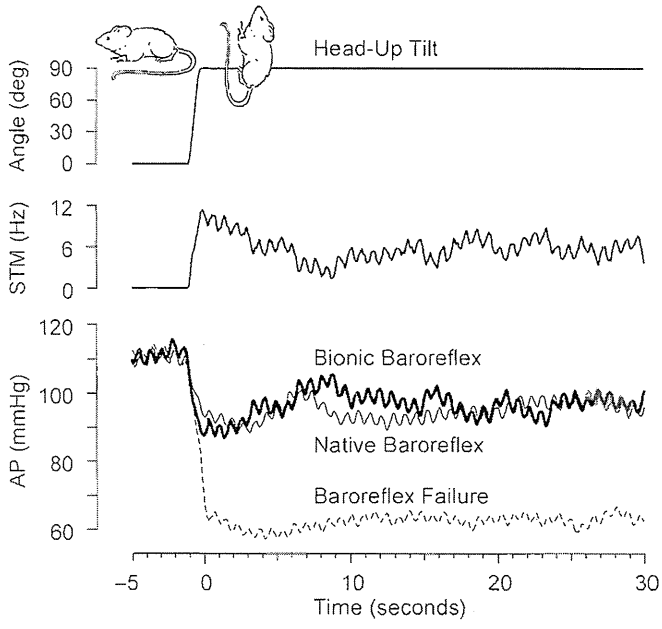

FIGURE 139.3 Real-time operation of the bionic baroreflex system during head-up tilting (HUT) in the rat. In a model of central baroreflex failure (broken line), when the bionic baroreflex system was inactive, arterial pressure (AP) fell rapidly and severely immediately after HUT. On the other hand, while the bionic baroreflex system was activated (thick line), such an AP fall was buffered, which was comparable to the native baroreflex (thin line). While sensing changes in AP, the bionic baroreflex system automatically computes the frequency of electrical stimulation (STM) of the sympathetic nerves and drives a stimulator. *(Modified from Sato et al. (2002) with permission of American Heart Association.)*

(H_{native}) is identified in normal subjects (Fig. 139.2). Second, the open-loop transfer function of the AP response to STM (H_{STM-AP}) is determined in patients with central baroreflex failure. Finally, a simple estimation process, H_{Native}/H_{STM-AP}, is used to yield the transfer function required for the artificial vasomotor center of the BBS, i.e., H_{AP-STM}.

Implementation of Algorithm of Artificial Vasomotor Center in BBS

To operate in real time as the artificial vasomotor center, the computer was programmed to automatically calculate instantaneous STM in response to instantaneous AP changes according to a convolution algorithm [2,3]:

$$STM(t) = \int_0^{\infty} h(\tau) \cdot AP(t - \tau)d\tau$$

where $h(t)$ is an impulse response function computed by an inverse Fourier transform of H_{AP-STM}.

Efficacy of BBS

In a prototype of the BBS for rats with central baroreflex failure, the celiac ganglion was selected as the sympathetic vasomotor interface [3]. The efficacy of the BBS against orthostatic hypotension during head-up tilting (HUT) is shown in Figure 139.3. Without the activation of the BBS, HUT produced a rapid progressive fall in AP by 40 mmHg in 2 seconds. In contrast, while the BBS was

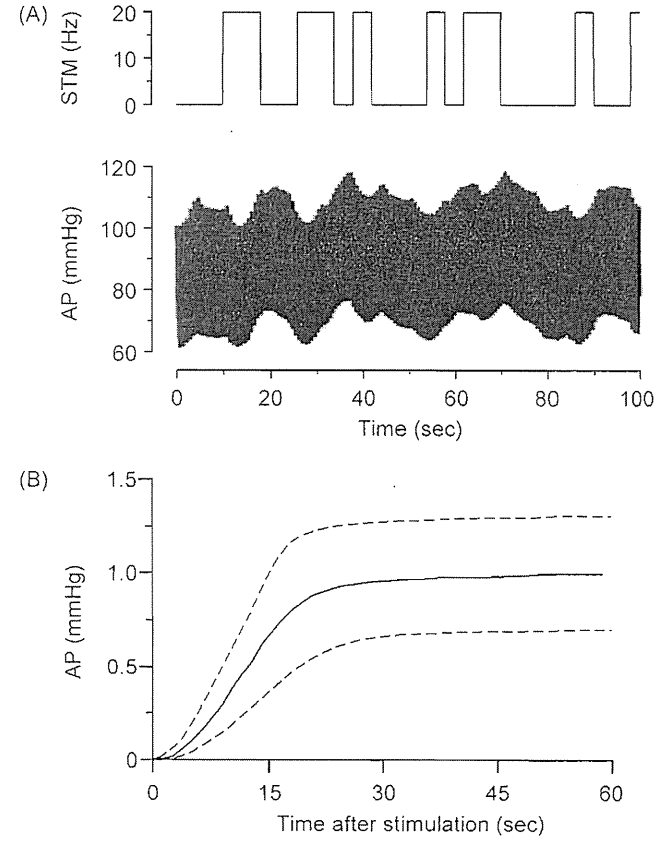

FIGURE 139.4 The response of arterial pressure (AP) to spinal cord stimulation at Th9-11 (A) and the step response estimated from the transfer function analysis (B).

activated, it automatically computed STM and appropriately stimulated the sympathetic nerves to quickly and effectively attenuate the AP drop. Such an AP response to HUT during the real-time execution of the BBS was indistinguishable from that observed in a control rat with an intact baroreflex system. Therefore, the BBS was considered to revitalize the native baroreflex function.

EPIDURAL CATHETER APPROACH FOR HUMAN BBS

To apply BIONIC technology to patients, we need a neural interface with quick and effective controllability of AP in humans. Here, we proposed an epidural catheter approach for the human BBS [4]. We percutaneously placed an epidural catheter with a pair of electrodes at the

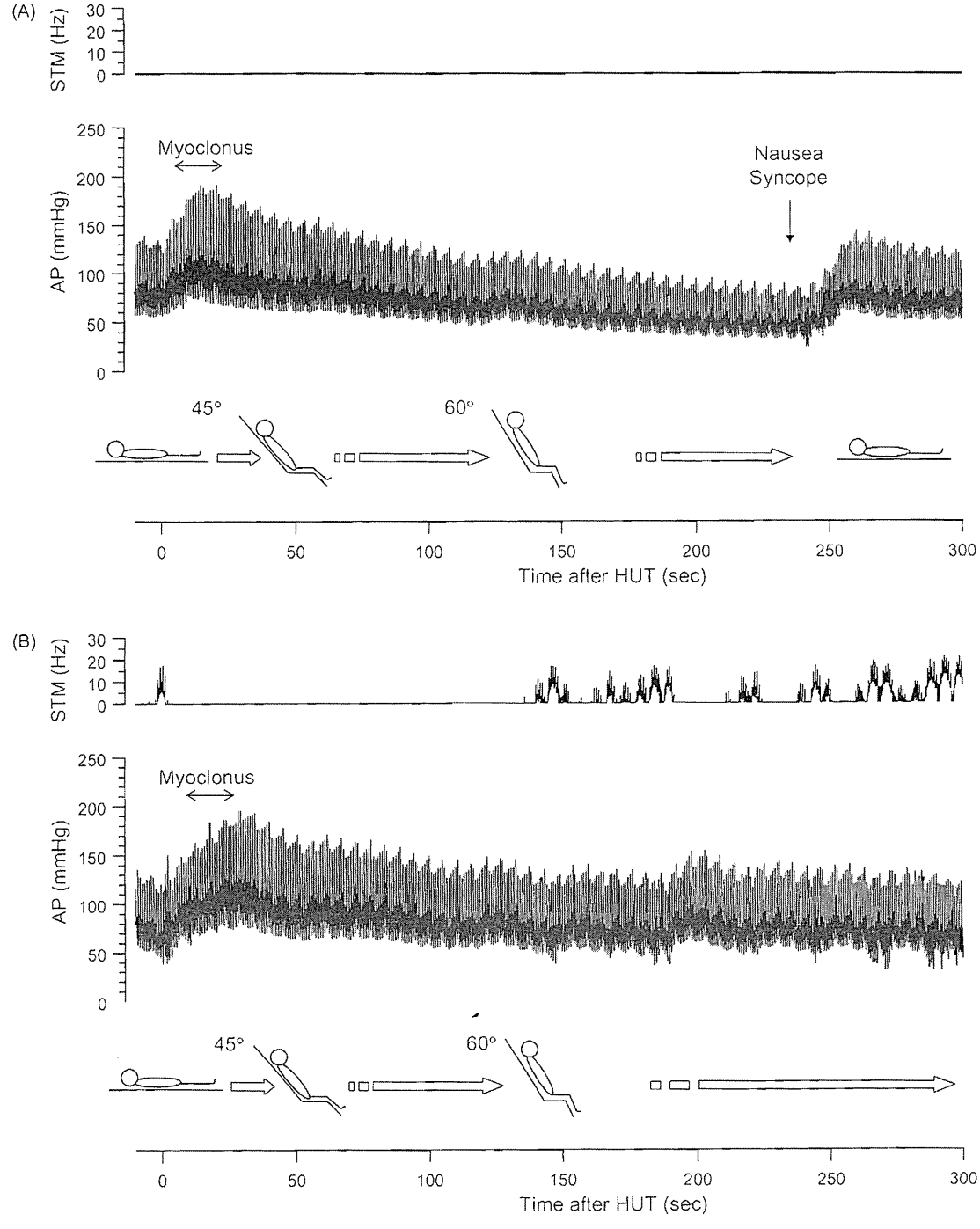

FIGURE 139.5 Clinical application of the bionic baroreflex system to a 55-year-old man with high cervical cord injury during head-up tilting (HUT). (A) Control; (B) Real-time operation of the bionic baroreflex system. *STM, stimulation frequency; AP, arterial pressure.*

level of Th9-11, and then we randomly altered the stimulation frequency between 0 and 20 Hz (Fig. 139.4A). The step response computed by the transfer function analysis showed that AP quickly responded to the electrical stimulation and reached 90% of the steady-state response at 21 ± 5 sec (Fig. 139.4B). The gain was 1.0 ± 0.3 mmHg/Hz. Therefore, the epidural approach would be a potential interface for the human BBS.

FEASIBLITY STUDY OF BBS IN PATIENTS WITH HIGH CERVICAL SPINAL CORD INJURY

A prototype of the clinical BBS with the epidural catheter electrodes [4] was developed and tested in some patients with high cervical spinal injury. A representative example is shown in Figure 139.5. HUT induced severe hypotension and syncope after transient AP elevation due to short myoclonus; however, the BBS prevented hypotension and enabled the subject to maintain a sitting position. The efficacy and safety of long-term use of the BBS should be investigated in the future.

IMPLANTABLE BBS

For practical use of the BBS for patients with central baroreflex failure, clinically applicable materials and devices should be developed, i.e., a pressure sensor, an implantable stimulator, and stimulating electrodes. Fortunately, certain difficulties posed by these challenges have already been addressed in other areas of clinical practice, and may be readily adaptable for use with the BBS. For example, a tonometer has been developed as a noninvasive continuous monitor of AP [5]. Implantable pulse generators such as cardiac pacemakers can serve as an electrical stimulator. Also, implantable wire leads for nerve stimulation and epidural catheters for spinal stimulation have been approved for the long-term treatment of some neurological disorders [6]. A future advance in development of the implantable BBS for assisting patients with difficulties in maintaining blood pressure during orthostatic maneuvers is expected in the future.

References

[1] Sato T, Kawada T, Inagaki M, Shishido T, Takaki H, Sugimachi M, et al. New analytic framework for understanding sympathetic baroreflex control of arterial pressure. Am J Physiol Heart Circ Physiol 1999;276:H2251–H2261.

[2] Sato T, Kawada T, Shishido T, Sugimachi M, Alexander Jr. J, Sunagawa K. Novel therapeutic strategy against central baroreflex failure: A bionic baroreflex system. Circulation 1999;100: 299–304.

[3] Sato T, Kawada T, Sugimachi M, Sunagawa K. Bionic technology revitalizes native baroreflex function in rats with baroreflex failure. Circulation 2002;106:730–4.

[4] Yamasaki F, Ushida T, Yokoyama T, Ando M, Yamashita K, Sato T. Artificial baroreflex: Clinical application of a bionic baroreflex system. Circulation 2006;113:634–9.

[5] Sato T, Nishinaga M, Kawamoto A, Ozawa T, Takatsuji H. Accuracy of a continuous blood pressure monitor based on arterial tonometry. Hypertension 1993;21:866–74.

[6] Shimoji K, Kitamura H, Ikezono E, Shimizu H, Okamoto K, Iwakura Y. Spinal hypalgesia and analgesia by low-frequency electrical stimulation in the epidural space. Anesthesiology 1974;41:91–4.

Clinical and Experimental Hypertension, 31:698–704, 2009

ISSN: 1064-1963 print / 1525-6006 online
DOI: 10.3109/10641960903407066

informa
healthcare

Atorvastatin Improves the Impaired Baroreflex Sensitivity via Anti-Oxidant Effect in the Rostral Ventrolateral Medulla of SHRSP

TAKUYA KISHI, YOSHITAKA HIROOKA, SATOMI KONNO, AND KENJI SUNAGAWA

Department of Cardiovascular Medicine, Kyushu University Graduate School of Medical Sciences, Fukuoka, Japan

We have demonstrated that oxidative stress in the rostral ventrolateral medulla (RVLM), a vasomotor center in brainstem, increases sympathetic nerve activity (SNA) and that oral administration of atorvastatin inhibited SNA via anti-oxidant effect in the RVLM of stroke-prone spontaneously hypertensive rats (SHRSPs). The impairment of baroreflex sensitivity (BRS) is known as the predictive factor of mortality in the hypertension and BRS is impaired in SHRSP. The aim of the present study was to determine whether oral administration of atorvastatin improved the impaired BRS via anti-oxidant effect in the RVLM in SHRSP. Atorvastatin (20 mg/kg/day) or vehicle was orally administered for 28 days in SHRSPs. Systolic blood pressure (SBP), heart rate, and 24-h urinary norepinephrine excretion as an indicator of SNA were comparable between atorvastatin- and control-SHRSP. Thiobarbituric acid-reactive substance (TBARS) levels as a marker of oxidative stress was significantly lower in atorvastatin-SHRSP than in control-SHRSP. Baroreflex sensitivity measured by the spontaneous sequence method was significantly higher in atorvastatin-SHRSP than in control-SHRSP. These results suggest that atorvastatin improves the impaired BRS in SHRSP via its anti-oxidant effect in the RVLM of SHRSP.

Keywords statin, oxidative stress, brain, hypertension, baroreflex

Introduction

Rostral ventrolateral medulla (RVLM) in the brainstem is the vasomotor center that determines basal sympathetic nerve activity, and the functional integrity of the RVLM is essential for the maintenance of basal vasomotor tone (1–3). We have demonstrated that oxidative stress in the RVLM increases the sympathetic nerve activity (4), and that nitric oxide (NO) in the RVLM decreases the sympathetic nerve activity (5,6). Previously, we also demonstrated that overexpression of endothelial NO synthase in the RVLM of Stroke-prone

Received August 31, 2008; revised November 11, 2008; accepted November 14, 2008.
Address correspondence to Takuya Kishi, Department of Cardiovascular Medicine, Kyushu University Graduate School of Medical Sciences, 3-1-1 Maidashi, Higashi-Ku, Fukuoka 812-8582, Japan; E-mail: tkishi@cardiol.med.kyushu-u.ac.jp

spontaneously hypertensive rats (SHRSPs) improved the baroreflex control of heart rate due to the sympatho-inhibition caused by the increase in NO production in the RVLM (7). However, it has not been determined whether the inhibition of oxidative stress in the RVLM improves the impaired baroreflex control of the heart rate of SHRSP or not.

The 3-hydroxy-3-methylglutaryl coenzyme A (HMG-CoA) reductase inhibitors (statins) are potent inhibitors of cholesterol biosynthesis, and statins have reported to have an anti-oxidant effect (8). Previously, we have demonstrated that orally atorvastatin increases the expression of NO synthase in the brain of SHRSPs (9), and that NO in the RVLM improves the impaired baroreflex control of heart rate in SHRSPs (7). These results suggested that orally atorvastatin might have the potential to improve the baroreflex control of heart rate in SHRSPs. Moreover, orally atorvastatin also inhibited the sympathetic nerve activity through the decrease in oxidative stress in the RVLM of SHRSPs (10).

Therefore, the aim of the present study was to investigate the effect of oral-administered atorvastatin on the baroreflex control of heart rate through its anti-oxidative stress in the RVLM of SHRSPs.

Materials and Methods

Animals and General Procedures

Twelve-week-old male SHRSPs/Izm and Wistar-Kyoto (WKY) rats (280 to 340g; SLC Japan, Hamamatsu, Japan) were fed a standard rodent diet. Food and tap water were available *ad libitum* throughout the study. The rats were kept in a room maintained at a constant temperature and humidity under a 12-h light period between 8:00 AM and 8:00 PM. After adaptation to these conditions over at least 2 weeks, SHRSPs were divided into two groups: 1) atorvastatin-treated SHRSP, treated with atorvastatin of 20mg/kg/day for 28 days, and 2) control-SHRSPs, treated with vehicle (0.5% methyl cellulose). All drugs were dissolved in 0.5% methyl cellulose and administered by gastric gavage everyday. Systolic blood pressure (SBP) and heart rate were measured using the tail-cuff method (BP-98A; Softron, Tokyo, Japan). We calculated the urinary norepinephrine excretion for 24 h as an indicator of sympathetic nerve activity, as described previously (4–7,10). To obtain the RVLM tissues, the rats were deeply anesthetized with sodium pentobarbital (100 mg/kg IP) and perfused transcardially with phosphate buffer saline (PBS) (150 mol/L NaCl, 3 mmol/L KCl, and 5 nmol/L phosphate; pH 7.4, 4°C). The brains were removed quickly, and sections 1 mm thick were obtained with a cryostat at -7 ± 1°C. The RVLM was defined according to a rat brain atlas as described previously (4–7,10), and obtained by a punch-out technique. This study was reviewed and approved by the committee on ethics of Animal Experiments, Kyushu University Graduate School of Medical Sciences, and conducted according to the Guidelines for Animal Experiments of Kyushu University.

Measurement of TBARS

The RVLM tissues were homogenized in 1.15% KCl (pH 7.4) and 0.4% sodium dodecyl sulfate, 7.5% acetic acid adjusted to pH 3.5 with NaOH. Thiobarbituric acid (0.3%) was added to the homogenate. The mixture was maintained at 5°C for 60 minutes, followed by heating to 100°C for 60 minutes. After cooling, the mixture was extracted with distilled water and *n*-butanolpyridine (15:1) and centrifuged at 1600 *g* for 10 minutes. The absorbance of the organic phase was measured at 532 nm. The amount of thiobarbituric acid-reactive substances (TBARS) was determined by absorbance, as described previously (4,10).

Measurement of Baroreflex Sensitivity by Spontaneous Sequence Method

Rats were initially anesthetized with sodium pentobarbital (50 mg/kg IP followed by 20 mg · kg^{-1} · h^{-1} IV). A catheter was inserted into the femoral artery to record arterial blood pressure, and a heart rate (HR) was derived from the blood pressure recording. The other catheter was also inserted into the femoral vein to allow for intravenous infusion of sodium pentobarbital. A tracheal cannula was connected to a ventilator, and the rats were artificially ventilated. Sequence analysis detected sequences of three or more beats in which there was an increase both in SBP and pulse interval (up sequence) or a decrease both in SBP and pulse interval (down sequence). Baroreflex sensitivity (BRS) was estimated as the mean slope of the up sequences (up BRS), the down sequences (down BRS), and also the mean slope of all sequences (sequence BRS) (11,12).

Statistical Analysis

All values are expressed as mean ± SEM. Comparisons between any two mean values were performed using Bonferroni's correction for multiple comparisons. ANOVA was used to compare the blood pressure, HR, baroreflex sensitivity, and TBARS level in atorvastatin- or control-SHRSP and WKY. Differences were considered to be statistically significant at a P value of < 0.05.

Results

BP, HR, and Urinary Norepinephrine Excretion

Systolic blood pressure was significantly higher in atorvastatin-SHRSP and control-SHRSP than in WKY, and atorvastatin did not alter SBP in SHRSP (Figure 1A). Heart rate was significantly higher in atorvastatin-SHRSP and control-SHRSP than in WKY, and atorvastatin also did not alter HR in SHRSP (Figure 1B). Urinary norepinephrine excretion was significantly higher in atorvastatin- and control-SHRSP than in WKY, and was not different between control- and atorvastatin-SHRSP (Figure 2).

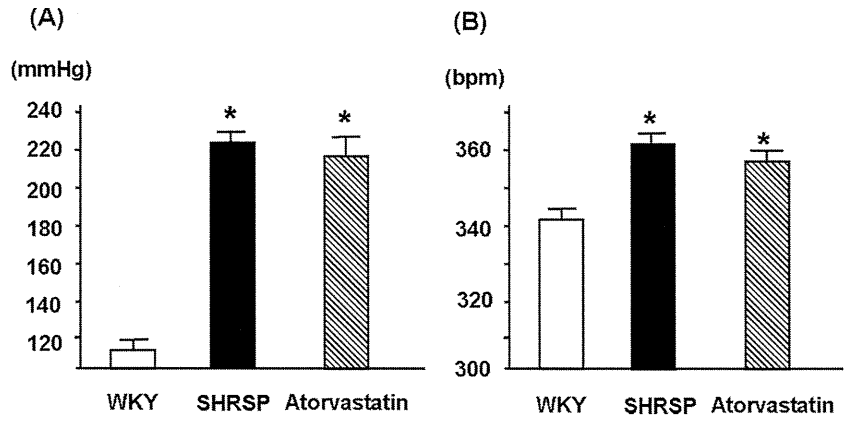

Figure 1. (A) Effects of the treatment with atorvastatin for 28 days on systolic blood pressure (SBP) of SHRSP and WKY. Data are shown as mean ± SEM (n = 5 for each group). *P < 0.05 vs. WKY. (B) Effects of the treatment with atorvastatin for 28 days on heart rate of SHRSP and WKY. Data are shown as mean ± SEM (n = 5 for each group). *P < 0.05 vs. WKY.

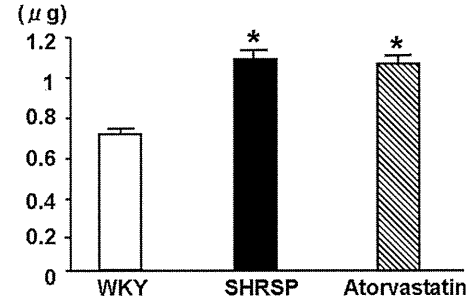

Figure 2. Effects of the treatment with atorvastatin for 28 days on 24-h urinary norepinephrine excretion of SHRSP and WKY. Data are shown as mean ± SEM (n = 5 for each group). *P < 0.05 vs. WKY.

TBARS Levels in the RVLM Tissues

Thiobarbituric acid-reactive substance levels in the RVLM were significantly higher in control- and atorvastatin-SHRSP than in WKY, and those of atorvastatin-SHRSP were significantly lower than those of control-SHRSP (0.70 ± 0.05 μmol/g wet wt vs. 0.91 ± 0.06 μmol/g wet wt, n = 5 for each, $P < 0.05$; Figure 3).

Baroreflex Sensitivity

Baroreflex sensitivity of control-SHRSP was significantly lower than that of WKY (9.2 ± 0.7 ms/mmHg vs. 19.1 ± 0.5 ms/mmHg, n = 5 for each, $P < 0.01$), and that of atorvastatin-SHRSP was significantly higher than that of control-SHRSP (14.8 ± 0.7 ms/mmHg vs. 9.2 ± 0.7 ms/mmHg, n = 5 for each, $P < 0.01$) (Figure 4).

Discussion

In the present study, we demonstrated for the first time that oral administration of atorvastatin improved the impaired baroreflex control of HR in SHRSP, and the improvement

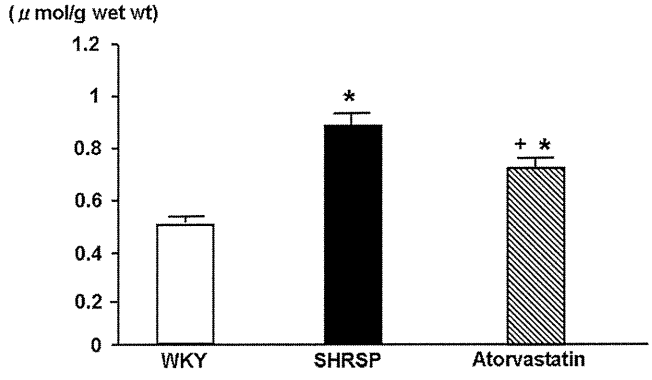

Figure 3. Effects of the treatment with atorvastatin for 28 days on TBARS levels in the RVLM of SHRSP and WKY. Data are shown as mean ± SEM (n = 5 for each group). *P < 0.05 vs. WKY; $^{+}$P < 0.05 vs. control-SHRSP.

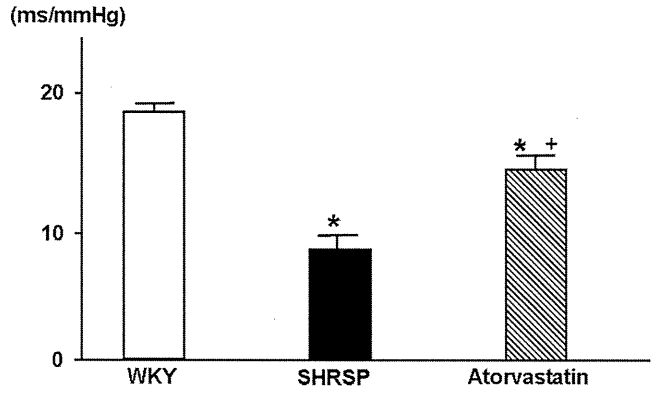

Figure 4. Effects of the treatment with atorvastatin for 28 days on baroreflex control of heart rate of SHRSP and WKY. Data are shown as mean ± SEM (n = 5 for each group). *P < 0.05 vs. WKY; $^{+}$P < 0.05 vs. control-SHRSP.

might be due in part to the inhibition of oxidative stress in the RVLM. Moreover, the improvement of baroreflex control of HR was independent of sympathetic nerve activity or blood pressure. We consider that these effects of atorvastatin benefit the treatment of the cardiovascular diseases with the disorder of baroreflex control.

In the present study, we demonstrated that atorvastatin improved the impaired baroreflex control without the reduction of BP or sympathetic nerve activity. Previously we reported that high-dose orally atorvastatin decreased BP and sympathetic nerve activity through the inhibition of oxidative stress in the RVLM (10). However, in the present study, low-dose atorvastatin did not decrease BP or sympathetic nerve activity, whereas oxidative stress in the RVLM was inhibited. We consider that this discrepancy is due to the smaller reduction of oxidative stress in the RVLM measure by TBARS compared to our previous study (10). We selected the lower dose of atorvastatin, because the effect of atorvastatin on baroreflex control should be examined in the condition excluded by BP and sympathetic nerve activity lowering effects. Moreover, baroreflex control is one of the key mechanisms responsible for the short-term control of BP. Impairment of this reflex has been found in a number of conditions, such as aging (13), heart failure (14), post-myocardial infarction (15), and the impairment of baroreflex sensitivity is known as the predictive factor of mortality in the hypertension (16). From the results in the present study, we consider that atorvastatin benefits the treatment for cardiovascular diseases.

The mechanisms in which atorvastatin improved the baroreflex control have not been determined in the present study. We consider that one of the possibilities in the mechanisms was the inhibition of oxidative stress in the RVLM, because the oxidative stress is the important modulator on the sympathetic nerve activity (4,10). Moreover, NO in the RVLM of SHRSPs improved the baroreflex control of HR (7). The inhibition of oxidative stress due to atorvastatin will contribute to the increase in NO in the RVLM of SHRSP and to the improvement of baroreflex control of HR.

A recent study suggests that the reduction of BP by clinical doses of statin is small but significant (17). However, the change in BP in the previous clinical study is significantly smaller than that in the present and previous animal study (10). Moreover, we are not able to determine the oxidative stress in the brain of human *in vivo* now and to determine whether the clinical doses of atorvastatin have the anti-oxidant effect in the

brain of the hypertensive patients. However, in the present study, oxidative stress in the RVLM is significantly reduced and baroreflex sensitivity is significantly improved by atorvastatin, whereas BP and sympathetic nerve activity are not altered. These results suggest that oxidative stress is inhibited and baroreflex sensitivity is improved by atorvastatin whose dose is insufficient for the reduction of blood pressure or sympathetic nerve activity. The improvement of baroreflex sensitivity could not be explained by the effect of atorvastatin on peripheral mechanisms, and we consider that baroreflex sensitivity is improved by the central action of atorvastatin. Clinical studies suggest that clinical doses of statins have the beneficial effect on arrhythmic sudden death and ventricular arrhythmia in the patients with heart failure, and these effects may be due to the improvement of the imbalance between sympathetic and parasympathetic nerve activity (18). It is necessary to examine the effect of clinical doses of atorvastatin on baroreflex sensitivity in a clinical study.

There are some limitations in the present study. First, we measured TBARS levels as the parameter of oxidative stress in the brain. Thiobarbituric acid-reactive substance levels are an indirect marker of oxidative stress, and there are other methods to measure oxidative stress. However, we previously measured oxidative stress directly in the brain of SHRSP and WKY using electron spin resonance spectroscopy and confirmed that TBARS levels are comparable to the levels of oxidative stress measured by electron spin resonance spectroscopy in the brain (4). The results suggest that TBARS levels are a valid parameter of oxidative stress in the brain. Second, we did not examine the TBARS levels in other areas of the brain, such as caudal ventrolateral medulla, nucleus tractus solitarii, paraventricular nucleus, cortex, hypothalamus, and cerebellum. We consider that these effects of atorvastatin was not unique in the RVLM, and we did not exclude the possibility that atorvastatin influences those areas thereby improving baroreflex control of HR in the present study. However, RVLM is the vasomotor center, and the integrated various inputs from other regions to RVLM influence the sympathetic outflow (1–3). Although it would be interesting to examine these parameters in other regions of the brain, we targeted the changes of oxidative stress in the RVLM due to atorvastatin in the present study.

Conclusions

Our results suggest that oral administration of atorvastatin improved the baroreflex control of heart rate due to the inhibition of oxidative stress in the RVLM of SHRSP.

Acknowledgments

We are grateful to Pfizer. USA, for supplying atorvastatin. This study was supported by a Grant-in-Aid for Scientific Research from the Japan Society for the Promotion of Science (B19390231), and in part, by the Health and Labor Sciences Research Grant for Comprehensive Research in Aging and Health Labor and Welfare of Japan.

Declaration of Interest

The authors report no conflicts of interest. The authors alone are responsible for the content and writing of the paper.

References

1. Dampney RA. Functional organization of central pathways regulating the cardiovascular system. *Physiol Rev* 1994;74:323–364.
2. Miyawaki T, Goodchild AK, Pilowsky PM. Evidence for a tonic GABA-ergic inhibition of excitatory respiratory-related afferents to presympathetic neurons in the rostral ventrolateral medulla. *Brain Res* 2002;924:56–62.
3. Guyenet PG. The sympathetic control of blood pressure. *Nat Rev Neurosci* 2006;7:335–346.
4. Kishi T, Hirooka Y, Kimura Y, Ito K, Shimokawa H, Takeshita A. Increased reactive oxygen species in rostral ventrolateral medulla contribute to neural mechanisms of hypertension in stroke-prone spontaneously hypertensive rats. *Circulation* 2004;109:3257–3262.
5. Kishi T, Hirooka Y, Sakai K, Shigematsu H, Shimokawa H, Takeshita A. Overexpression of eNOS in the RVLM causes hypotension and bradycardia via GABA release. *Hypertension* 2001;38:896–901.
6. Kishi T, Hirooka Y, Ito K, Sakai K, Shimokawa H, Takeshita A. Cardivascular effects of overexpression of endothelial nitric oxide synthase in the rostral ventrolateral medulla in stroke-prone spontaneously hypertensive rats. *Hypertension* 2002;39:264–268.
7. Kishi T, Hirooka Y, Kimura Y, Sakai K, Ito K, Shimokawa H, Takeshita A. Overexpression of eNOS in RVLM improves impaired baroreflex control of heart rate in SHRSP. *Hypertension* 2003;41:255–260.
8. Laufs U, La Fata V, Plutzky J, Liao JK. Upregulation of endothelial nitric oxide synthase by HMG-CoA reductase inhibitors. *Circulation* 1998; 97:1129–1135.
9. Kishi T, Hirooka Y, Mukai Y, Shimokawa H, Takeshita H. Atorvastatin causes depressor and sympatho-inhibitory effects with upregulation of nitric oxide synthase in stroke-prone spontaneously hypertensive rats. *J Hypertens* 2003;21:379–386.
10. Kishi T, Hirooka Y, Shimokawa H, Takeshita A, Sunagawa K. Atorvastatin reduces oxidative stress in the rostral ventrolateral medulla in stroke-prone spontaneously hypertensive rats. *Clin Exp Hypertens* 2008;30:1–9.
11. Waki H, Kasparov S, Wong LF, Murphy D, Shimizu T, Paton JFR. Chronic inhibition of eNOS activity in nucleus tractus solitarii enhances baroreceptor reflex in conscious rats. *J Physiol* 2003;546:233–242.
12. Waki H, Katahira K, Polson JW, Kasparov S, Murphy D, Paton JFR. Automation of analysis of cardiovascular autonomic function from chronic measurements of arterial pressure in conscious rats. *Exp Physiol* 2006;91:201–213.
13. Latinen T, Hartikainen J, Vanninen E, Niskanen L, Geelen G, Lansimies E. Age and gender dependency of baroreflex sensitivity in healthy subjects. *J Appl Physiol* 1998;84:576–583.
14. Mortara A, La Rovere MT, Pinna GD, Prpa A, Maestri R, Fedo O, Pozzoli M, Opasich C, Tavazzi L. Arterial baroreflex modulation of heart rate in chronic heart failure: Clinical and hemodynamic correlates and prognostic implications. *Circulation* 1997;96:3450–3458.
15. Farrell TG, Odemuyiwa O, Bashir Y, Gripps TR, Malik M, Ward DE, Camm AJ. Prognostic value of baroreflex sensitivity testing after acute myocardial infarction. *Br Heart J* 1992; 67:129–137.
16. Hesse C, Charkoudian N, Liu Z, Joyner MJ, Eisenach JH. Baroreflex sensitivity inversely correlates with ambulatory blood pressure in healthy normotensive humans. *Hypertension* 2007;50:41–46.
17. Golomb BA, Dimsdale JE, White HL, Ritchie JB, Criqui MH. Reduction in blood pressure with statins: Results from the USCD Statin Study, a randomized trial. *Arch Intern Med* 2008;168:721–727.
18. Goldberger JJ, Subacius H, Schaechter A, Howard A, Berger R, Shalaby A, Levine J, Kadish AH: DEFINITE Investigators. Effects of statin therapy on arrhythmic events and survival in patients with nonischemic dilated cardiomyopathy. *J Am Coll Cardiol* 2006;48:1228–1233.

31st Annual International Conference of the IEEE EMBS
Minneapolis, Minnesota, USA, September 2-6, 2009

Bionic Autonomic Neuromodulation Revolutionizes Cardiology in the 21st Century

Kenji Sunagawa, *Senior Member, IEEE*

Abstract — **In this invited session, we would like to address the impact of bionic neuromodulation on cardiovascular diseases. It has been well established that cardiovascular dysregulation plays major roles in the pathogenesis of cardiovascular diseases. This is the reason why most drugs currently used in cardiology have significant pharmacological effects on the cardiovascular regulatory system. Since the ultimate center for cardiovascular regulation is the brainstem, it is conceivable that autonomic neuromodulation would have significant impacts on cardiovascular diseases. On the basis of this framework, we first developed a bionic, neurally regulated artificial pacemaker. We then substituted the brainstem by CPU and developed a bionic artificial baroreflex system. We further developed a bionic brain that achieved better regulatory conditions than the native brainstem in order to improve survival in animal model with heart failure. We recently developed a bionic neuromodulation system to reduce infarction size following acute myocardial infarction. We believe that the bionic neuromodulation will inspire even more intricate applications in cardiology in the 21st century.**

I. OVERVIEW OF PREVIOUIS BIONIC STUDIES

In the human body, all cells, tissues, organs, and systems operate coherently. The presence of well-developed neurohormonal communications among these components of the body is the essential infrastructure that makes coherent functioning possible. If we could incorporate such communication mechanisms into artificial systems, they would function as if they are an integral part of the corresponding native physiological systems. We call such well-integrated artificial systems bionic systems.

The bread-and-butter technology that is common to all bionic systems is the technique for interfacing with the native systems, in particular, the human body's regulatory systems. Unification of an artificial system with a native system requires bidirectional communications. In 1995, we developed one such system, a neurally regulated artificial pacemaker [1]. Physiological studies indicated that the instantaneous sinus rate was determined not only by the current sympathetic activity but also by the history of sympathetic activity. We quantified its history dependence by the impulse response of the sinus rate to sympathetic stimulation. Using the convolution integral of the impulse response with the instantaneous sympathetic activity, we could predict the precise sinus rate in real time [1].

The success of the neurally regulated bionic pacemaker has convinced us that the autonomic system can be effectively monitored and thereby manipulated by bionic systems. The clinical impact of direct manipulation of autonomic functions in cardiovascular diseases is very profound. The case of central baroreflex failure is an archetypal example of one such application. In treating this disease, it is conceivable that one can implement an artificial bionic baroreflex system as a kind of biological proxy capable of emulating the native central baroreflex function of the failing vasomotor center. The bionic baroreflex system consists of a pressure sensor (baroreceptor), microprocessor (vasomotor center) and nerve stimulator (for activation of sympathetic efferents). The system operates as an intelligent negative feedback regulator, and has been demonstrated in animals and patients to be effective in restoring normal baroreflex functioning [2-5].

Recently, we developed an artificial brain stem that takes over the native cardiac regulation, and optimized it to improve the survival of chronic heart failure [6]. Two weeks after the ligation of the left coronary artery in rats, surviving animals were randomized to vagal- and sham-stimulated groups. Vagal stimulation markedly improved the 140-day survival (86% versus 50%, P=0.008). The relative risk reduction of death reached over 70%. The success of the bionic treatment of heart failure opens up an entirely new therapeutic paradigm for patients with chronic heart failure.

II. BIONIC NEUROMODULATION IN ISCHEMIA

Although the bionic autonomic neuromodulation system prevented progression, thereby improved survival of chronic heart failure, it would be far desirable if we can prevent the development of heart failure. Ischemic heart disease has been known as one of the major causes of heart failure. Therefore, we examined whether bionic autonomic neuromodulation impacts ischemia-reperfusion injury of the heart. This particular application of bionic autonomic neuromodulation is critically important under clinical settings because early reperfusion of occluded coronary arteries has become a standard therapy worldwide.

Myocardial infarction has been known to augment sympathetic afferent traffic and reduce vagal efferent activity. We investigated whether short-term electrical stimulation of

978-1-4244-3296-7/09/$25.00 ©2009 IEEE

the vagal nerve could ameliorate cardiac dysfunction in a distant period after ischemia-reperfusion injury.

Ischemia-reperfusion injury model was created in Sprague-Dawley rats by ligating the left coronary artery for 30 min followed by reperfusion. We stimulated the right vagal nerve (the stimulation condition is proprietary) from the onset of ischemia for 3 hrs. We measured hemodynamics before ischemia, 4 days after ischemia with and without bionic autonomic neuromodulation. We estimated left ventricular function using echocardiography. We estimated infarction size histologically 4 days after ischemia.

III. RESULTS

As shown in the upper panels of figure, in comparison with sham stimulation (SS, n=6), vagal nerve stimulation (VNS, n=6) significantly decreased left ventricular end-diastolic pressure, and increased left ventricular (dp/dt)max suggesting improved left ventricular function. CNT represents the control condition (n=4). The improvement of left ventricular function was paralleled with decreased end-diastolic dimension (EDD), and increased shortening fraction (EF) as shown in the lower panels in the figure. Histological examination further supported the notion that vagal stimulation decreased the infarction size (33±5% vs. 24±3%, $p<.01$). Biochemical analysis indicated that vagal stimulation downregulated mRNA of procollagens, such as Col1a1, Col3a1, and Ctgf, in infarcted myocardium. Therefore, the positive impact of vagal nerve stimulation might have, at least in part, resulted from inhibition of collagen production in ischemia-reperfusion injury.

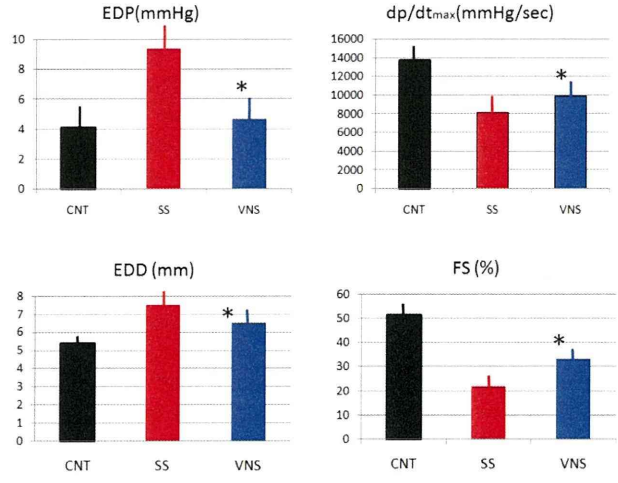

IV. DISCUSSION

We have shown that vagal stimulation early after the creation of ischemia resulted in marked reduction in infarction size and improvement of left ventricular function with attenuated cardiac remodeling. Although the effect of vagal nerve stimulation on long term survival remains to be investigated, it is conceivable that the vagal nerve stimulation early after ischemia-reperfusion injury may have a positive impact on such a hard endpoint.

The mechanism by which the bionic neuromodulation improves ischemia-reperfusion injury remains unknown. The bradycardiac effect of vagal stimulation might be a contributing factor. However, our pilot study indicated that a comparable heart rate reduction induced by beta-blocker failed to show the positive impacts on ischemia-reperfusion injury as much as the vagal stimulation did. Theretofore, mechanisms other than the bradycardiac effect such as energy sparing effect, anti-inflammatory effect and anti-oxidant effect need to be considered [7-10].

V. CONCLUSION

Vagal nerve stimulation reduces infarct size, improves left ventricular function and attenuates left ventricular remodeling after ischemia-reperfusion injury. Bionic autonomic neuromodulation should inspire even more intricate applications in cardiology in the 21st century.

REFERENCES

[1] Y. Ikeda, M. Sugimachi, T. Yamasaki, O. Kawaguchi, T. Shishido, T. Kawada, J. Jr. Alexander, and K. Sunagawa, "Explorations into development of a neurally regulated cardiac pacemaker," *Am J Physiol*, vol. 269, pp. 2141-6, Dec 1995.

[2] T. Sato, T. Kawada, M. Inagaki, T. Shishido, H. Takaki, M. Sugimachi, and K. Sunagawa, "New analytic framework for understanding sympathetic baroreflex control of arterial pressure," *Am J Physiol*, vol. 276, pp. H2251-61, Jun 1999.

[3] T. Sato, T. Kawada, T. Shishido, M. Sugimachi, J. Alexander, Jr., and K. Sunagawa, "Novel therapeutic strategy against central baroreflex failure: a bionic baroreflex system," *Circulation*, vol. 100, pp. 299-304, Jul 20 1999.

[4] T. Sato, T. Kawada, M. Sugimachi, and K. Sunagawa, "Bionic technology revitalizes native baroreflex function in rats with baroreflex failure," *Circulation*, vol. 106, pp. 730-4, Aug 6 2002.

[5] Y. Yanagiya, T. Sato, T. Kawada, M. Inagaki, T. Tatewaki, C. Zheng, A. Kamiya, H. Takaki, M. Sugimachi, and K. Sunagawa, "Bionic epidural stimulation restores arterial pressure regulation during orthostasis." *J Appl Physiol*, vol. 97, pp.984-990, Sep 2004.

[6] M. Li, C. Can, T. Sato, M. Sugimachi, and K. Sunagawa, "vagal nerve stimulation markedly improves long-term survival after chronic heart failure in rats," *Circulation*, vol 109, pp 120-124, 2004

[7] T. Tsutsumi, T. Ide, M. Yamato, M. Andou, T. Shiba, H. Utsumi, and K. Sunagawa, "Effect of anesthesia-induced alterations in hemodynamics on in vivo kinetics of nitroxyl probes in electron spin

resonance spectroscopy," *Free Radic Res,*. Vol. 42, pp. 305-11, Apr 2008.

[8] T. Tsutsumi, T. Ide, M. Yamato, W. Kudou , M. Andou, Y. Hirooka, H. Utsumi, H. Tsutsui, and K. Sunagawa. "Modulation of the myocardial redox state by vagal nerve stimulation after experimental myocardial infarction," *Cardiovasc Res,* vol. 77, pp.713-721, Mar 1, 2008.

[9] K. Uemura, M. Li, T. Tsutsumi, T. Yamazaki, T. Kawada, A. Kamiya, M. Inagaki, K. Sunagawa and M. Sugimachi, "Efferent vagal nerve stimulation induces tissue inhibitor of metalloproteinase-1 in myocardial ischemia-reperfusion injury in rabbit." *Am J Physiol*, vol. 293, pp H2254-H2261, Oct, 2008.

[10] T. Inoue, T. Ide, M. Yamato, M. Yoshida, T. Tsutsumi, M. Andou, H. Utsumi, H. Tsutsui, and K. Sunagawa, "Time-dependent changes of myocardial and systemic oxidative stress are dissociated after myocardial infarction," *Free Radic Res,* Vol. 43, pp.37-46, Jan 2009.

Inhibition of Prolyl Hydroxylase Domain-Containing Protein Suppressed Lipopolysaccharide-Induced TNF-α Expression

Kotaro Takeda, Toshihiro Ichiki, Eriko Narabayashi, Keita Inanaga, Ryohei Miyazaki, Toru Hashimoto, Hirohide Matsuura, Jiro Ikeda, Toshio Miyata, Kenji Sunagawa

Objective—Prolyl hydroxylase domain-containing proteins (PHDs) play pivotal roles in oxygen-sensing system through the regulation of α-subunit of hypoxia-inducible factor (HIF), a key transcription factor governing a large set of gene expression to adapt hypoxia. Although tissue hypoxia plays an essential role in maintaining inflammation, the role of PHDs in the inflammatory responses has not been clearly determined. Here, we investigated the role of PHDs in lipopolysaccharide (LPS)-induced tumor necrosis factor α (TNF-α) induction in macrophages.

Methods and Results—Northern blot analysis and ELISA revealed that LPS-induced TNF-α upregulation was strongly suppressed by PHD inhibitors, dimethyloxallyl glycine (DMOG), and TM6008 in RAW264.7 macrophages. DMOG suppressed LPS-induced TNF-α upregulation in HIF-1α–depleted cells and HIF-1α overexpression failed to suppress the induction of TNF-α. DMOG rather suppressed LPS-induced NF-κB transcriptional activity. Downregulation of *Phd1* or *Phd2* mRNA by RNA interference partially attenuated LPS-induced TNF-α induction. DMOG also inhibited LPS-induced TNF-α production in peritoneal macrophages as well as human macrophages.

Conclusions—PHD inhibition by DMOG or RNA interference inhibited LPS-induced TNF-α upregulation in macrophages possibly through NF-κB inhibition, which is independent of HIF-1α accumulation. This study suggests that PHDs are positive regulators of LPS-induced inflammatory process, and therefore inhibition of PHD may be a novel strategy for the treatment of inflammatory diseases. (***Arterioscler Thromb Vasc Biol.* 2009;29:2132-2137.)**

Key Words: tumor necrosis factor -alpha ■ prolyl hydroxylase domain-containing protein ■ hypoxia-inducible factor ■ inflammation ■ hypoxia

Inflammation is a fundamental process for the protection of our body against outside pathogen. Tissues with inflammation are characterized by several features including the accumulation of inflammatory cells such as macrophages, lymphocytes, and neutrophils, limited blood supply attributable to impaired local microcirculation, and abnormal angiogenesis.[1] Inflammatory cells are metabolically active and consume a large amount of oxygen and nutrient. These cells are, therefore, eventually exposed to hypoxic and nutrient-deprived condition.[2] Thus, the inflammatory cells need to adapt these hypoxic conditions to perpetuate inflammatory reaction.[3]

The reduced oxygen concentration is directly sensed by an innate oxygen-sensing system.[4–6] The hypoxia-inducible factor (HIF) is a key transcription factor that mediates cellular adaptive responses to hypoxia.[7] HIF is a heterodimer consisting of an oxygen-labile α-subunit and a stable β-subunit. The stability of the α-subunit of HIF-1 and HIF-2 (HIF-1α and HIF-2α) is regulated through the hydroxylation at the 4-position of specific proline residues in HIF-1α and HIF-2α by prolyl hydroxylase domain-containing proteins (PHDs).[8,9] Because PHD activity depends on the availability of molecular oxygen, PHDs are able to serve as a sensor for oxygen concentration. Under normal oxygen concentration, HIF-α is well hydroxylated by PHDs and tagged by von Hipple-Lindau (VHL) E3 ubiquitin ligase complex to be targeted for proteosomal degradation.[8,9] When oxygen concentration is reduced, the activity of PHDs is decreased. This results in the accumulation of HIF in the nucleus, followed by upregulation of a series of genes suited for hypoxic condition.

Because hypoxia is closely associated with an inflammatory reaction, it is reasonable that HIF is essential to maintain inflammatory processes. By switching energy production from oxidative phosphorylation to an anaerobic metabolism, macrophages generate ATP and thereby preserve its bactericidal ability in the hypoxic tissues.[10,11] HIF-1α–deficient myeloid cells showed impaired inflammatory responses attributable to inefficient energy production.[10,12] In contrast to HIF, the role of PHD in the inflammation is somewhat controversial. A specific knockdown of *Phd* gene led to the activation of NF-κB and hence upregulation of proinflamma-

Received May 17, 2009; revision accepted September 3, 2009.

From the Departments of Advanced Therapeutics for Cardiovascular Diseases (K.T., T.I., K.S.) and Cardiovascular Medicine (E.N., K.I., R.M., T.H., H.M., J.I., K.S.), Kyushu University Graduate School of Medical Sciences, Fukuoka, Japan; and the Center for Translational and Advanced Research (T.M.), Tohoku University Graduate School of Medicine, Miyagi, Japan.

Correspondence to Toshihiro Ichiki, MD, PhD, Department of Cardiovascular Medicine, Kyushu University Graduate School of Medical Sciences, 3-1-1, Maidashi, Higashi-ku, 812-8582 Fukuoka, Japan. E-mail ichiki@cardiol.med.kyushu-u.ac.jp

Arterioscler Thromb Vasc Biol **is available at http://atvb.ahajournals.org** **DOI: 10.1161/ATVBAHA.109.196071**

tory molecules in HeLa cells.[13] On the other hand, chemical PHD inhibitors attenuated inflammatory responses in several models including colitis and myocardial inflammation after an ischemic insult.[14–16] Thus, in the present study, we focused on the question whether PHD inhibition suppresses or activates inflammatory responses in macrophages. We demonstrated that the PHD inhibition by pharmacological inhibitors or RNA interference suppressed lipopolysaccharide (LPS)-elicited induction of tumor necrosis factor α (TNF-α),[17] a pivotal proinflammatory cytokine. However, interestingly the suppression was mediated not by a HIF-α accumulation but by suppression of NF-κB transcriptional activity. Our data suggest that suppression of PHD may be a novel antiinflammatory mechanism.

Methods

To clarify the role of PHD inhibition on inflammatory response, murine macrophage cell line, RAW264.7 cells were stimulated with LPS in the presence or absence of PHD inhibitor. The effect of LPS on mouse peritoneal macrophage, and human monoctye cell line, THP-1 was also examined. PHD isoforms were selectively knocked down by stable transfection of small hairpin RNA expression vector. Expression of TNF-α and other inflammatory cytokines were examined by quantitative reverse-transcription PCR (qPCR) or Northern blot analysis. Promoter activity was examined by luciferase assay. Nuclear translocation of NF-κB was examined by electrophoretic mobility shift assay and ELISA-based TransAM NF-κB p65 Transcription Factor Assay Kits. Cell viability was measured by flow cytometry after propidium iodide statining.

Detailed information of materials and methods used in this article is available in the online Data Supplement (please see http://atvb.ahajournals.org).

Results

DMOG Suppressed LPS-Induced TNF-α Upregulation in Macrophages

To assess the effect of the PHD inhibition on inflammatory response, RAW264.7 macrophages were pretreated with a vehicle DMSO or DMOG (1 mmol/L) for 1 hour before 100 ng/mL of LPS stimulation. Real-time qPCR and Northern blot analysis revealed that DMOG time- and dose-dependently inhibited LPS-induced *Tnf-α* mRNA upregulation (Figure 1A and 1B and supplemental Figure IA and IB). TNF-α secretion in the supernatant during 24 hours of LPS treatment was also suppressed by DMOG (Figure 1C).

A luciferase gene regulated by murine *Tnf-α* gene promoter was introduced into the RAW264.7 cells, and luciferase activity was measured. A LPS treatment (100 ng/mL for 6 hours) significantly increased *Tnf-α* promoter activity and DMOG significantly suppressed the upregulation (Figure 1D). In contrast, DMOG did not affect *Tnf-α* mRNA stability (data not shown). We tested another novel PHD inhibitor, TM6008.[18] Pretreatment with TM6008 (100 μmol/L) for 1 hour significantly suppressed TNF-α secretion in the supernatant after 24 hours of LPS treatment (supplemental Figure II). In addition to TNF-α, DMOG suppressed LPS-induced TNF-α converting enzyme (*Tace*) expression (supplemental Figure III).

Phd Knockdown Strongly Attenuated the LPS-Induced Cytokine Production

To examine whether the suppressive effect of DMOG is indeed mediated by the PHD inhibition, *Phd* gene expression

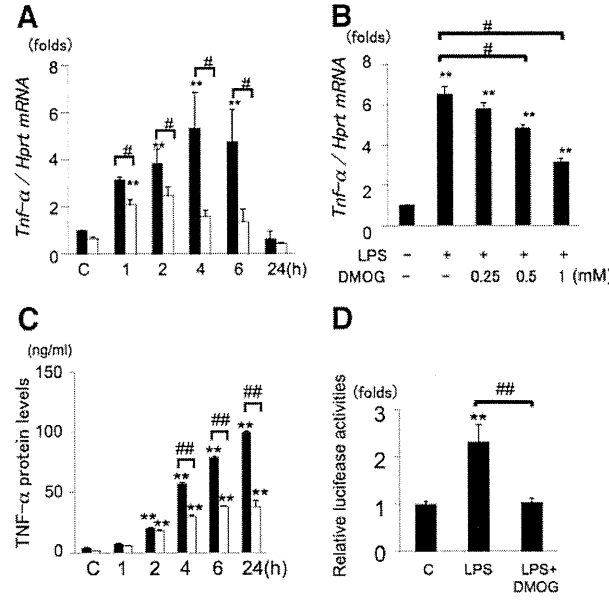

Figure 1. DMOG suppressed LPS-induced TNF-α upregulation in RAW264.7 macrophages. A, After pretreatment with 1 mmol/L of DMOG (open bar) or a vehicle DMSO (filled bar) for 1 hour, RAW264.7 cells were stimulated with LPS (100 ng/mL) for varying periods indicated in the figure. *Tnf-α* mRNA was determined by real-time qPCR. B, The effect of varying concentrations of DMOG pretreatment for 1 hour on LPS (100 ng/mL, 4 hours)-induced *Tnf-α* mRNA expression was examined. *Tnf-α* mRNA level was normalized with the level of *Hprt* mRNA. C, TNF-α concentration in the supernatant of RAW264.7 cells during 24 hours of LPS (100 ng/mL) treatment with the pretreatment of 1 mmol/L of DMOG (open bar) or a vehicle DMSO (filled bar) for 1 hour was determined by ELISA. D, LPS-induced *Tnf-α* gene promoter activity after 100 ng/mL of LPS treatment for 6 hours with pretreatment of 1 mmol/L of DMOG or DMSO for 1 hour was measured as luciferase activity. n=3 to 4. $^{**}P<0.01$ vs control, $\#P<0.05$, $\#\#P<0.01$ vs LPS (alone).

was knocked down by shRNA introduction. Because there are at least three PHD isoforms (PHD1, PHD2, and PHD3) in mice,[19] we determined the expression of *Phd* isoforms in RAW264.7 macrophages. Real-time qPCR analyses revealed that *Phd3* gene was expressed at very low level in RAW264.7 cells (Figure 2A). We, therefore, downregulated *Phd1* and *Phd2* expression by shRNA. *Phd1* and *Phd2* shRNA efficiently decreased *Phd1* and *Phd2* mRNA expression by 91±1% and 67±2%, respectively (Figure 2B). Although *Phd2* shRNA did not affect *Phd1* mRNA expression, *Phd1* shRNA increased *Phd2* mRNA expression by 1.4-fold (Figure 2B). Then, these *Phd1*- or *Phd2*-depleted cells were stimulated with 100 ng/mL of LPS. LPS-induced *Tnf-α* mRNA upregulation and TNF-α secretion were significantly inhibited in both *Phd1*- and *Phd2*-depleted cells (Figure 2C and 2D and Figure IV). However, *Phd1* depletion showed stronger suppression of *Tnf-α* expression than *Phd2* depletion.

Activation of HIF Pathway by DMOG or *Phd2* Knockdown but not by *Phd1* Knockdown

To confirm whether the DMOG inhibition of PHD activates the HIF pathway in RAW264.7 macrophages, the levels of 2 main HIF-α isoforms (HIF-1α and HIF-2α) were determined

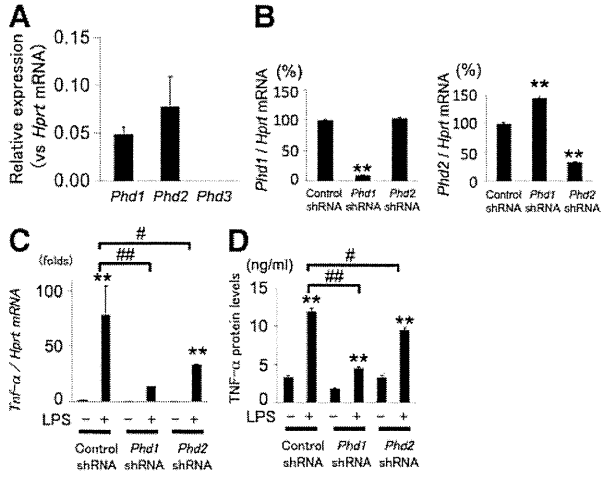

Figure 2. *Phd* knockdown suppressed LPS-induced TNF-α upregulation in RAW264.7 macrophages. A, The expression of *Phd1–3* mRNA was analyzed by real-time qPCR. B, The expression of *Phd1* or *Phd2* mRNA in control or *Phd1*- or *Phd2*-specific shRNA expressing cells was analyzed by real-time qPCR. C, Real-time qPCR analysis for *Tnf-α* mRNA in *Phd1*- or *Phd2*-depleted cells with or without LPS stimulation (100 ng/mL, 4 hours). D, ELISA for TNF-α concentration in the supernatant was performed in *Phd1*- or *Phd2*-depleted cells with or without LPS stimulation (100 ng/mL, 24 hours). n=3 to 4. #$P<0.05$, ##$P<0.01$ vs LPS (alone), **$P<0.01$ vs control or LPS (−).

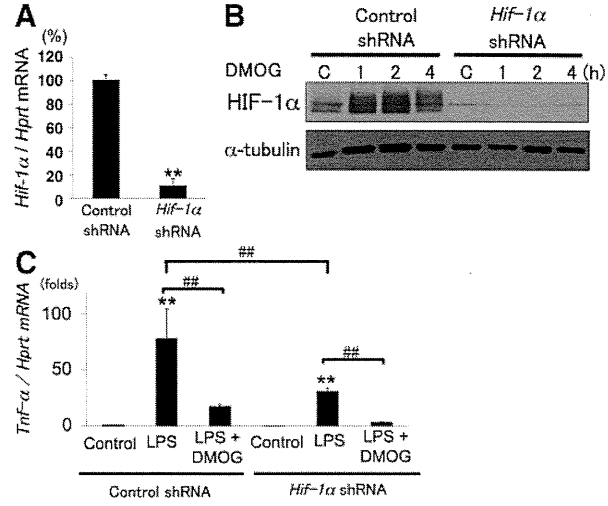

Figure 4. DMOG suppressed LPS-induced *Tnf-α* upregulation in HIF-1α–depleted macrophages. A, *Hif-1α* mRNA expression was determined by real-time qPCR. B, Western blot analysis for HIF-1α in control or *Hif-1α* shRNA expressing RAW264.7 cells after 1 mmol/L of DMOG treatment for varying periods indicated in the figure. The same results were obtained in other 2 independent experiments. C, LPS (100 ng/mL, 4 hours)-stimulated *Tnf-α* expression in control or *Hif-1α* shRNA expressing cells with pretreatment of 1 mmol/L of DMOG or a vehicle DMSO for 1 hour was determined by real-time qPCR. n=3 to 4. **$P<0.01$ vs control, ##$P<0.01$.

by Western blot analyses. Whereas HIF-1α was dramatically accumulated by DMOG treatment, HIF-2α protein remained undetectable (Figure 3A). Western blot for HIF-2α was validated by clear detection of HIF-2α expression in placenta lysate as a positive control.[20] A HRE-driven luciferase

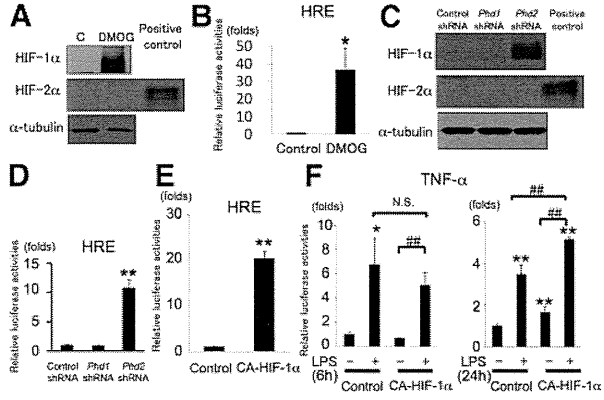

Figure 3. Expression of CA-HIF-1α failed to suppress LPS-induced *Tnf-α* upregulation. A and C, Western blot analysis for HIF-1α and HIF-2α after DMOG treatment (1 mmol/L, 6 hours) in RAW264.7 cells (A) or in *Phd1* or *Phd2* shRNA expressing RAW264.7 cells (C). The same results were obtained in 2 other independent experiments. Murine placenta total lysate was used as a positive control for HIF-2α. B and D, HRE-luciferase activities were measured in RAW264.7 cells with 1 mmol/L of DMOG or a vehicle DMSO for 24 hours (B) and in control, *Phd1*, or *Phd2* shRNA expressing RAW264.7 cells (D). E, The luciferase activity of HRE-luciferase vector after 24 hours of cotransfection with CA-HIF-1α expression vector or empty vector was measured. n=3. F, The *Tnf-α* gene promoter-luciferase activity after 24 hours of CA-HIF-1α vector or empty vector introduction followed by 6 or 24 hours of 100 ng/mL of LPS stimulation was measured. n=3 to 4. NS indicates not statistically significant, *$P<0.05$, **$P<0.01$ vs LPS (−) or control, ##$P<0.01$.

expression vector[21] was transiently introduced and a luciferase activity was measured. DMOG treatment for 24 hours strongly increased the HRE-dependent transcriptional activity (Figure 3B).

We also determined the levels of HIF-α in *Phd1*- or *Phd2*-depleted cells. Introduction of *Phd2* shRNA, but not *Phd1* shRNA, induced HIF-1α accumulation, whereas HIF-2α was not induced by either *Phd1* or *Phd2* shRNA (Figure 3C). HRE-dependent transcriptional activity was only increased in *Phd2*-depleted cells (Figure 3D).

A HIF-1α Overexpression Failed to Suppress the LPS-Induced *Tnf-α* Promoter Activation

To test whether accumulated HIF-1α by DMOG is responsible for the suppression of LPS-induced TNF-α induction, we determined the effect of overexpression of CA-HIF-1α.[22] The expression of CA-HIF-1α strongly increased HRE-dependent transcriptional activity (Figure 3E). However, *Tnf-α* gene transcriptional activity was not suppressed in CA-HIF-1α–expressing cells after 6 hours or 24 hours of LPS stimulation (Figure 3F).

DMOG Suppressed LPS-Induced *Tnf-α* Upregulation in *Hif-1α*–Depleted Cells

We next examined whether DMOG would be able to suppress the LPS-induced *Tnf-α* upregulation in the absence of HIF-1α. shRNA specific for *Hif-1α* gene strongly decreased the *Hif-1α* mRNA level and the DMOG-induced HIF-1α accumulation (Figure 4A and 4B). Then, *Hif-1α*–depleted cells were pretreated with DMOG for 1 hour and stimulated with 100 ng/mL of LPS for 4 hours. Consistent with a previous report,[12] the induction of *Tnf-α* mRNA was significantly

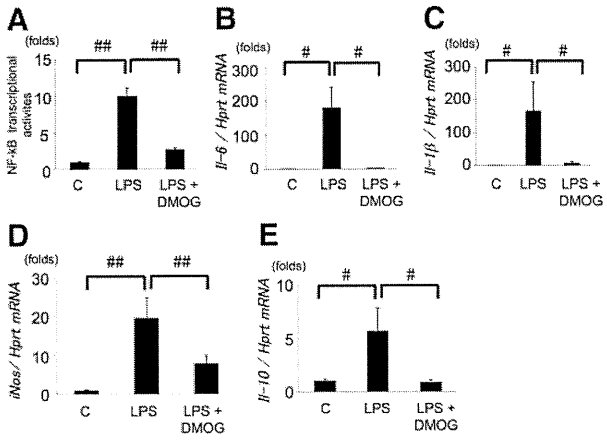

Figure 5. DMOG treatment suppressed LPS-induced NF-κB transcriptional activation and upregulation of other cytokines. A, LPS-induced NF-κB transcriptional activity after 8 hours of LPS treatment with pretreatment of 1 mmol/L of DMOG or DMSO for 1 hour was measured as luciferase activity. n=3. B through E, RAW264.7 macrophages were stimulated with 100 ng/mL of LPS for 4 hours with DMOG or DMSO pretreatment for 1 hour. The expressions of *Il-6* (B), *Il-1β* (C), *iNos* (D), and *Il-10* (E) were determined by real-time qPCR and normalized with the expression level of *Hprt* gene. n=4. #$P<0.05$, ##$P<0.01$.

reduced in *Hif-1α*–depleted cells (Figure 4C). However, DMOG further suppressed the LPS-induced *Tnf-α* upregulation in *Hif-1α*–depleted cells (Figure 4C and supplemental Figure V).

DMOG Treatment Suppressed LPS-Induced NF-κB Transcriptional Activation

Because both activation of NF-κB and mitogen-activated protein kinases (MAP kinases) is responsible for the LPS-induced TNF-α induction,[23] we examined whether DMOG would suppress an activation of MAP kinases such as p38, c-Jun N-terminal kinase (JNK), and extracellular signal-regulated kinase (ERK). Phosphorylation of these kinases, a surrogate marker of kinase activation, was strongly induced by 100 ng/mL of LPS but the activation was not reduced by DMOG pretreatment (supplemental Figure VIA through VIC).

Next, LPS-induced activation of NF-κB transcriptional activity was determined with NF-κB–dependent luciferase activity. LPS treatment for 8 hours strongly increased NF-κB transcriptional activity and DMOG pretreatment significantly suppressed the activation (Figure 5A). NF-κB nuclear translocation and binding capacity to NF-κB consensus site were determined by electrophoretic mobility shift assay and ELISA-based DNA-binding assay by using nuclear protein extract after LPS stimulation, respectively. However, translocation of NF-κB into the nucleus and binding capacity to NF-κB site was not decreased by DMOG pretreatment (supplemental Figure VIIA and VIIB).

The Effect of DMOG on Other Cytokine Productions

We examined the effect of DMOG on LPS-induced expression of other genes encoding inducible nitric oxide synthase (iNOS), proinflammatory cytokines (eg, interleukin [IL]-6, IL-1β) and antiinflammatory cytokine (eg, IL-10), of which

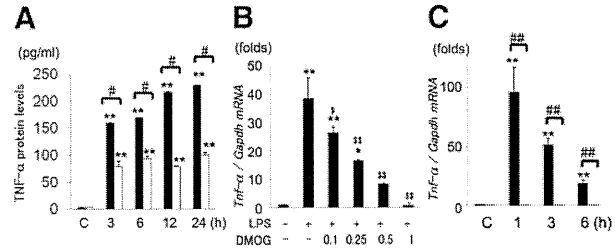

Figure 6. DMOG suppressed LPS-induced TNF-α upregulation in murine peritoneal macrophages and human THP-1 macrophages. A, Peritoneal macrophages from normal mice were stimulated with 100 ng/mL of LPS for varying periods indicated in the figure with pretreatment of 1 mmol/L of DMOG (open bar) or a vehicle DMSO (filled bar) for 1 hour. TNF-α concentration in the supernatant was determined by ELISA. n=3 to 4. B, Human THP-1 macrophages were stimulated with 100 ng/mL of LPS for 1 hour after pretreatment with varying concentrations of DMOG for 1 hour. *Tnf-α* mRNA level was determined by real-time qPCR and normalized with *Gapdh* mRNA levels. C, THP-1 cells were stimulated with 100 ng/mL of LPS for varying periods indicated in the figure with pretreatment of 1 mmol/L of DMOG (open bar) or a vehicle DMSO (filled bar) for 1 hour. #$P<0.05$, ##$P<0.01$, **$P<0.01$ vs control, \$$P<0.05$, \$\$$P<0.01$ vs LPS.

expression is dependent on NF-κB. DMOG significantly suppressed LPS-induced upregulation of these genes (Figure 5B through 5E). Because all cytokines studied were suppressed by DMOG, we excluded the possible cytotoxic effect of DMOG. Flow cytometry to detect PI-positive dead cells revealed that 1 mmol/L of DMOG treatment for 24 hours did not affect cell viability in RAW264.7 macrophages (supplemental Figure VIII). The cytotoxic effect of DMOG was further ruled out by the evidence that DMOG upregulated *Vegf* gene expression (supplemental Figure IX).

DMOG Suppressed LPS-Induced TNFα Upregulation in Resident Peritoneal Macrophages and Human THP-1

Finally, to generalize the effect of DMOG on LPS-induced TNF-α upregulation, we analyzed the effect of DMOG on 2 different types of macrophages. One is murine peritoneal macrophages from normal mice, and the other is human monocyte cell line THP-1. Consistent with the results of RAW264.7 macrophages, DMOG pretreatment significantly suppressed LPS-induced TNF-α secretion in peritoneal macrophages (Figure 6A). DMOG also time- and dose-dependently suppressed LPS-induced *Tnf-α* mRNA upregulation in differentiated THP-1 macrophages (Figure 6B and 6C).

Discussion

In this article, we demonstrated that PHD inhibition by DMOG significantly suppressed LPS-induced expression of several proinflammatory genes encoding not only TNF-α but IL-6, IL-1β, iNOS, and antiinflammatory gene IL-10 in macrophages. Although DMOG treatment apparently raised HIF-1α level, the increased HIF-1α was not responsible for the suppression. And PHD1 among three PHD isoforms may be mainly responsible for the suppressive effect of DMOG on LPS function. These data indicated that PHD inhibition decreased cellular sensitivity to inflammatory stimuli and may have a therapeutic implication.

How does PHD inhibition suppress LPS-induced TNF-α upregulation? Because PHD is a negative regulator for HIF-1α or HIF-2α expression, one would expect that increased HIF-α might be responsible for the suppression. HIF-2α was undetectable in RAW264.7 macrophages, excluding the possible involvement of HIF-2α. In contrast, DMOG strongly induced HIF-1α accumulation and activated HRE-dependent transcription. However, DMOG suppressed LPS-induced *Tnf-α* upregulation even in *Hif-1α*–depleted cells. Moreover, *Phd1* knockdown significantly inhibited LPS-elicited TNF-α upregulation but did not increase HIF-1α levels. In addition, forced expression of stable form of HIF-1α (CA-HIF-1α) failed to inhibit TNF-α promoter activity. These evidences consistently indicate that DMOG-mediated suppression of the LPS effect does not depend on HIF-1α as well as HIF-2α.

The mechanism by which PHD inhibition attenuated LPS-induced TNF-α production is not clear at this point, but several possibilities may be considered. First of all, because NF-κB activation is an essential step for the induction of cytokines such as TNF-α, IL-6, IL-1β, iNOS, and antiinflammatory IL-10,[24,25] DMOG-induced NF-κB suppression may be a potential mechanism. We observed that DMOG did not suppress nuclear translocation or binding capacity to NF-κB consensus site but reduced NF-κB–dependent transcriptional activity. The mechanism by which DMOG suppressed NF-κB activation remains elusive. However, recent studies suggest that phosphorylation of NF-κB on Ser536 phosphorylation is essential for the NF-κB transcriptional activation.[26] Thus, DMOG may affect the phosphorylation of NF-κB to suppress LPS-induced transcriptional activation.

In contrast to our data, a previous report suggest that DMOG may enhance inflammatory reaction. Cummins et al described that PHD-induced hydroxylation of IκB kinase-β (IKKβ), an activator of NF-κB pathway, attenuated its kinase activity.[13] DMOG activates NF-κB pathway and induces proinflammatory cyclooxygenase 2 expression in HeLa cells.[13] The reason for the discrepancy between their study and ours is not immediately clear, but it may be possible that PHD inhibition causes different effects on different cell type, which is most likely reflecting differential expression pattern of PHD isoforms.[19,27] Alternatively, DMOG may increase the basal expression of proinflammatory genes[13] while decreasing the induction of these genes on inflammatory stimuli. Therefore, further study is needed to clarify the effect of PHD inhibition in several different experimental conditions of inflammation.

Other possible mechanisms for DMOG-elicited suppression of LPS-induced TNF-α upregulation may be the suppression of oxidative phosphorylation and global energy consumption. DMOG treatment significantly inhibits electron transport chain activity during mitochondrial respiration, leading to the reduced ATP production in cardiomyocytes.[28] DMOG also inhibits intracellular ATP consumption, an example of which is the reduction of contraction in cardiomyocytes.[28] Therefore, DMOG may suppress energy metabolism, leading to attenuation of inflammatory responses in macrophages.

Our isoform-specific knockdown experiments indicated that PHD1 was mainly responsible for LPS-induced TNF-α upregulation. In IKKβ hydroxylation, PHD1 is also mainly responsible.[13] PHD1 knockout mice caused reduced ATP production and consumption in skeletal muscle.[29] These data indicate that although PHD2 is generally important for HIF regulation,[30] PHD1 might have a distinct pathway rather than HIF to regulate various biological activities. Thus, further study is needed to identify a target molecule of hydroxylation by PHD1 to clarify the role of PHD1 in LPS-induced inflammation. In this study, we did not analyze the role of PHD3, because PHD3 was not expressed in RAW264.7 cells. However, PHD3 has a potential to compensate the role of PHD1 in other cells that express PHD3.[31] Thus, we cannot exclude the possible involvement of PHD3 in other inflammatory models in which PHD3 is present substantially.

In general, hypoxia is considered to induce or augment inflammatory responses. For instance, hypoxia augments LPS-induced TNF-α and iNOS expression in several cell lines including RAW264.7 macrophages and murine dendritic cells.[32–34] Thus, it may be counterintuitive that PHD inhibition suppresses LPS-induced TNF-α expression, because both hypoxia and PHD inhibition induce HIF-α accumulation and upregulation of HIF target gene expression. However, the biological effects caused by hypoxia or PHD inhibition are not necessarily the same or even opposite.[29] One example is a production of reactive oxygen species (ROS); hypoxia increases ROS production, whereas PHD inhibition decreases ROS.[29] If hypoxia-induced ROS production potentiates inflammation, reduced ROS production by PHD inhibition may attenuate inflammation. Thus, it is possible that hypoxia and PHD inhibition induce opposite biological responses in some cases. Our study indicates that PHD inhibition suppresses LPS-induced TNF-α upregulation, which is usually augmented by hypoxic exposure.[32,33]

Taken together, we provided the first-line evidence that PHD inhibition suppressed LPS-induced proinflammatory TNF-α production independently of HIF-1α in macrophages. TNF-α is involved in various pathological conditions, including sepsis, autoimmune disorders, atherosclerosis, and obesity-associated insulin resistance.[12,35,36] Antagonizing TNF-α has been shown to be protective for several inflammatory diseases.[37] Therefore, PHD inhibition might be a novel strategy for the treatment of inflammatory diseases.

Acknowledgments

The authors would like to acknowledge the technical expertise of the Support Center for Education and Research, Kyushu University.

Sources of Funding

This work was supported in part by a Grant-in-Aid for Scientific Research from the Ministry of Education, Culture, Sports, Science, and Technology of Japan (21790731) and Japan Heart Foundation/Novartis Grant for Research Award on Molecular and Cellular Cardiology (2008) to K.T.

Disclosures

None.

References

1. Larsen GL, Henson PM. Mediators of inflammation. *Annu Rev Immunol.* 1983;1:335–359.
2. Zinkernagel AS, Johnson RS, Nizet V. Hypoxia inducible factor (HIF) function in innate immunity and infection. *J Mol Med.* 2007;85: 1339–1346.
3. Murdoch C, Muthana M, Lewis CE. Hypoxia regulates macrophage functions in inflammation. *J Immunol.* 2005;175:6257–6263.
4. Kaelin WG Jr, Ratcliffe PJ. Oxygen sensing by metazoans: the central role of the HIF hydroxylase pathway. *Mol Cell.* 2008;30:393–402.
5. Bruick RK, McKnight SL. A conserved family of prolyl-4-hydroxylases that modify HIF. *Science.* 2001;294:1337–1340.
6. Epstein AC, Gleadle JM, McNeill LA, Hewitson KS, O'Rourke J, Mole DR, Mukherji M, Metzen E, Wilson MI, Dhanda A, Tian YM, Masson N, Hamilton DL, Jaakkola P, Barstead R, Hodgkin J, Maxwell PH, Pugh CW, Schofield CJ, Ratcliffe PJ. *C. elegans* EGL-9 and mammalian homologs define a family of dioxygenases that regulate HIF by prolyl hydroxylation. *Cell.* 2001;107:43–54.
7. Semenza GL. Targeting HIF-1 for cancer therapy. *Nat Rev Cancer.* 2003;3:721–732.
8. Ivan M, Kondo K, Yang H, Kim W, Valiando J, Ohh M, Salic A, Asara JM, Lane WS, Kaelin WG Jr. HIFalpha targeted for VHL-mediated destruction by proline hydroxylation: implications for O2 sensing. *Science.* 2001;292:464–468.
9. Jaakkola P, Mole DR, Tian YM, Wilson MI, Gielbert J, Gaskell SJ, Kriegsheim A, Hebestreit HF, Mukherji M, Schofield CJ, Maxwell PH, Pugh CW, Ratcliffe PJ. Targeting of HIF-alpha to the von Hippel-Lindau ubiquitylation complex by O2-regulated prolyl hydroxylation. *Science.* 2001;292:468–472.
10. Cramer T, Yamanishi Y, Clausen BE, Forster I, Pawlinski R, Mackman N, Haase VH, Jaenisch R, Corr M, Nizet V, Firestein GS, Gerber HP, Ferrara N, Johnson RS. HIF-1alpha is essential for myeloid cell-mediated inflammation. *Cell.* 2003;112:645–657.
11. Peyssonnaux C, Datta V, Cramer T, Doedens A, Theodorakis EA, Gallo RL, Hurtado-Ziola N, Nizet V, Johnson RS. HIF-1alpha expression regulates the bactericidal capacity of phagocytes. *J Clin Invest.* 2005;115: 1806–1815.
12. Peyssonnaux C, Cejudo-Martin P, Doedens A, Zinkernagel AS, Johnson RS, Nizet V. Cutting edge: Essential role of hypoxia inducible factor-1alpha in development of lipopolysaccharide-induced sepsis. *J Immunol.* 2007;178:7516–7519.
13. Cummins EP, Berra E, Comerford KM, Ginouves A, Fitzgerald KT, Seeballuck F, Godson C, Nielsen JE, Moynagh P, Pouyssegur J, Taylor CT. Prolyl hydroxylase-1 negatively regulates IkappaB kinase-beta, giving insight into hypoxia-induced NFkappaB activity. *Proc Natl Acad Sci U S A.* 2006;103:18154–18159.
14. Cummins EP, Seeballuck F, Keely SJ, Mangan NE, Callanan JJ, Fallon PG, Taylor CT. The hydroxylase inhibitor dimethyloxalylglycine is protective in a murine model of colitis. *Gastroenterology.* 2008;134: 156–165.
15. Robinson A, Keely S, Karhausen J, Gerich ME, Furuta GT, Colgan SP. Mucosal protection by hypoxia-inducible factor prolyl hydroxylase inhibition. *Gastroenterology.* 2008;134:145–155.
16. Natarajan R, Salloum FN, Fisher BJ, Ownby ED, Kukreja RC, Fowler AA III. Activation of hypoxia-inducible factor-1 via prolyl-4 hydoxylase-2 gene silencing attenuates acute inflammatory responses in postischemic myocardium. *Am J Physiol Heart Circ Physiol.* 2007;293: H1571–H1580.
17. Carmody RJ, Chen YH. Nuclear factor-kappaB: activation and regulation during toll-like receptor signaling. *Cell Mol Immunol.* 2007;4:31–41.
18. Nangaku M, Izuhara Y, Takizawa S, Yamashita T, Fujii-Kuriyama Y, Ohneda O, Yamamoto M, van Ypersele de Strihou C, Hirayama N, Miyata T. A novel class of prolyl hydroxylase inhibitors induces angiogenesis and exerts organ protection against ischemia. *Arterioscler Thromb Vasc Biol.* 2007;27:2548–2554.
19. Lieb ME, Menzies K, Moschella MC, Ni R, Taubman MB. Mammalian EGLN genes have distinct patterns of mRNA expression and regulation. *Biochem Cell Biol.* 2002;80:421–426.
20. Takeda K, Ho VC, Takeda H, Duan LJ, Nagy A, Fong GH. Placental but Not Heart Defects Are Associated with Elevated Hypoxia-Inducible Factor {alpha} Levels in Mice Lacking Prolyl Hydroxylase Domain Protein 2. *Mol Cell Biol.* 2006;26:8336–8346.
21. Katavetin P, Miyata T, Inagi R, Tanaka T, Sassa R, Ingelfinger JR, Fujita T, Nangaku M. High glucose blunts vascular endothelial growth factor response to hypoxia via the oxidative stress-regulated hypoxia-inducible factor/hypoxia-responsible element pathway. *J Am Soc Nephrol.* 2006; 17:1405–1413.
22. Kelly BD, Hackett SF, Hirota K, Oshima Y, Cai Z, Berg-Dixon S, Rowan A, Yan Z, Campochiaro PA, Semenza GL. Cell type-specific regulation of angiogenic growth factor gene expression and induction of angiogenesis in nonischemic tissue by a constitutively active form of hypoxia-inducible factor 1. *Circ Res.* 2003;93:1074–1081.
23. Tominaga K, Saito S, Matsuura M, Nakano M. Lipopolysaccharide tolerance in murine peritoneal macrophages induces downregulation of the lipopolysaccharide signal transduction pathway through mitogen-activated protein kinase and nuclear factor-kappaB cascades, but not lipopolysaccharide-incorporation steps. *Biochim Biophys Acta.* 1999; 1450:130–144.
24. Guha M, Mackman N. LPS induction of gene expression in human monocytes. *Cell Signal.* 2001;13:85–94.
25. Liu YW, Chen CC, Tseng HP, Chang WC. Lipopolysaccharide-induced transcriptional activation of interleukin-10 is mediated by MAPK- and NF-kappaB-induced CCAAT/enhancer-binding protein delta in mouse macrophages. *Cell Signal.* 2006;18:1492–1500.
26. Cui R, Tieu B, Recinos A, Tilton RG, Brasier AR. RhoA mediates angiotensin II-induced phospho-Ser536 nuclear factor kappaB/RelA subunit exchange on the interleukin-6 promoter in VSMCs. *Circ Res.* 2006;99:723–730.
27. Appelhoff RJ, Tian YM, Raval RR, Turley H, Harris AL, Pugh CW, Ratcliffe PJ, Gleadle JM. Differential Function of the Prolyl Hydroxylases PHD1, PHD2, and PHD3 in the Regulation of Hypoxia-inducible Factor. *J Biol Chem.* 2004;279:38458–38465.
28. Sridharan V, Guichard J, Li CY, Muise-Helmericks R, Beeson CC, Wright GL. O(2)-sensing signal cascade: clamping of O(2) respiration, reduced ATP utilization, and inducible fumarate respiration. *Am J Physiol Cell Physiol.* 2008;295:C29–C37.
29. Aragones J, Schneider M, Van Geyte K, Fraisl P, Dresselaers T, Mazzone M, Dirkx R, Zacchigna S, Lemieux H, Jeoung NH, Lambrechts D, Bishop T, Lafuste P, Diez-Juan A, Harten SK, Van Noten P, De Bock K, Willam C, Tjwa M, Grosfeld A, Navet R, Moons L, Vandendriessche T, Deroose C, Wijeyekoon B, Nuyts J, Jordan B, Silasi-Mansat R, Lupu F, Dewerchin M, Pugh C, Salmon P, Mortelmans L, Gallez B, Gorus F, Buyse J, Sluse F, Harris RA, Gnaiger E, Hespel P, Van Hecke P, Schuit F, Van Veldhoven P, Ratcliffe P, Baes M, Maxwell P, Carmeliet P. Deficiency or inhibition of oxygen sensor Phd1 induces hypoxia tolerance by reprogramming basal metabolism. *Nat Genet.* 2008;40:170–180.
30. Berra E, Benizri E, Ginouves A, Volmat V, Roux D, Pouyssegur J. HIF prolyl-hydroxylase 2 is the key oxygen sensor setting low steady-state levels of HIF-1alpha in normoxia. *EMBO J.* 2003;22:4082–4090.
31. Takeda K, Aguila HL, Parikh NS, Li X, Lamothe K, Duan LJ, Takeda H, Lee FS, Fong GH. Regulation of adult erythropoiesis by prolyl hydroxylase domain proteins. *Blood.* 2008;111:3229–3235.
32. Liu FQ, Liu Y, Lui VC, Lamb JR, Tam PK, Chen Y. Hypoxia modulates lipopolysaccharide induced TNF-alpha expression in murine macrophages. *Exp Cell Res.* 2008;314:1327–1336.
33. Jantsch J, Chakravortty D, Turza N, Prechtel AT, Buchholz B, Gerlach RG, Volke M, Glasner J, Warnecke C, Wiesener MS, Eckardt KU, Steinkasserer A, Hensel M, Willam C. Hypoxia and hypoxia-inducible factor-1 alpha modulate lipopolysaccharide-induced dendritic cell activation and function. *J Immunol.* 2008;180:4697–4705.
34. Mi Z, Rapisarda A, Taylor L, Brooks A, Creighton-Gutteridge M, Melillo G, Varesio L. Synergystic induction of HIF-1alpha transcriptional activity by hypoxia and lipopolysaccharide in macrophages. *Cell Cycle.* 2008;7: 232–241.
35. Hansson GK, Libby P. The immune response in atherosclerosis: a double-edged sword. *Nat Rev Immunol.* 2006;6:508–519.
36. Xu H, Barnes GT, Yang Q, Tan G, Yang D, Chou CJ, Sole J, Nichols A, Ross JS, Tartaglia LA, Chen H. Chronic inflammation in fat plays a crucial role in the development of obesity-related insulin resistance. *J Clin Invest.* 2003;112:1821–1830.
37. Shealy DJ, Visvanathan S. Anti-TNF antibodies: lessons from the past, roadmap for the future. *Handb Exp Pharmacol.* 2008;181:101–129.